



14<sup>TH</sup> CANADIAN MASONRY SYMPOSIUM  
MONTREAL, CANADA  
MAY 16<sup>TH</sup> – MAY 20<sup>TH</sup>, 2021



---

SHAKE-TABLE TESTS ON COLLAPSE RESISTANCE OF REINFORCED MASONRY  
WALL SYSTEMS

Cheng, Jianyu<sup>1</sup>; Koutras, A. Andreas<sup>2</sup> and Shing, P. Benson<sup>3</sup>

**ABSTRACT**

Shake-table tests were performed to investigate the displacement capacity of shear-dominated reinforced masonry wall systems and the influence of wall flanges and planar walls perpendicular to the direction of shaking (out-of-plane walls) on the seismic performance of a wall system. Two full-scale, single-story, fully grouted, reinforced masonry wall specimens were tested to the verge of collapse. Each specimen had two T-walls as the seismic force-resisting elements and a stiff roof diaphragm. The second specimen had six additional out-of-plane walls. The two specimens reached maximum roof drift ratios of 17% and 13%, without collapsing. The high displacement capacities can be largely attributed to the presence of wall flanges and, for the second specimen, the out-of-plane walls, which provided an alternative load path to carry the gravity load when the webs of the T-walls had been severely damaged. The maximum lateral resistance developed in the first specimen was close to predicted shear strength given by the formula in TMS 402/602. However, the maximum lateral resistance developed in the second specimen was 18% higher than predicted, which can be attributed to the additional axial compression exerted on the T-walls by the out-of-plane walls when the former rocked.

**KEYWORDS:** *reinforced masonry, shear failure, displacement capacity, collapse resistance, shake table*

---

<sup>1</sup> Ph.D Candidate, Department of Structural Engineering, University of California, San Diego, La Jolla, CA, USA.  
j7cheng@eng.ucsd.edu

<sup>2</sup> Postdoctoral Rresearcher, Department of Structural Engineering, University of California, San Diego, La Jolla, CA, USA. akoutras@ucsd.edu

<sup>3</sup> Professor, Department of Structural Engineering, University of California, San Diego, La Jolla, CA, USA.  
pshing@ucsd.edu

## INTRODUCTION

For the design of reinforced masonry (RM) wall systems in high seismic areas, the value of the seismic force modification factor ( $R$ ) is based on the expectation that the walls can develop sufficient flexural ductility to sustain a significant amount of story drifts without collapsing when subjected to severe seismic forces. Nevertheless, in spite of the reinforcement and shear capacity design requirements in TMS 402/602 [1] for special RM walls, such wall systems could still develop shear-dominated behavior when there are wall components with low shear-span ratios. This could be the case for perforated wall systems, or wall systems that have unintended coupling forces exerted by horizontal diaphragms, which will significantly reduce the shear-span ratio of the walls.

The behavior and lateral resistance of shear-dominated reinforced masonry walls have been studied by many researchers. Voon and Ingham [2], Shing et al. [3], and Ahmadi [4] conducted quasi-static tests on shear-dominated single wall segments. The test results showed that walls with shear-dominated behavior were significantly more brittle than flexure-dominated walls. Although the above observations have raised concerns about the safety of buildings that may be susceptible to shear-dominated wall failures, past shake-table tests showed that fully grouted RM wall systems with shear-dominated wall components could develop drift capacity much higher than that would normally be expected. The two-story wall system tested by Mavros et al. [5] showed a 20% strength degradation at a maximum first-story drift ratio of 2%. Similarly, the three-story structure tested by Stavridis et al. [6] had a 27% strength degradation at a maximum first-story drift of 1.6%. The ductile behavior observed in the two wall systems could be attributed to the beneficial influence of wall flanges. Furthermore, other walls or columns that are present in the structural system to carry gravity loads could enhance the lateral resistance of the shear walls and the displacement capacity of the system by providing axial restraints as well as alternative load paths for gravity loads. However, the exact influence of the wall flanges and other components in a wall system on the behavior of walls dominated by diagonal shear cracks is not well understood.

This paper presents a study to investigate the displacement capacity of shear-dominated fully grouted RM wall systems and the influence of wall flanges and planar walls perpendicular to the direction of the seismic force on the seismic performance of a wall system. To this end, two full-scale, single-story, RM wall systems were tested on a shake table to the verge of collapse. The tests were carried out with unidirectional base excitation. The paper presents the design of the two structures, the test setup, and the major results and findings from the shake-table tests.

## DESIGN OF TEST STRUCTURES

Figure 1 shows the plan layouts of the two RM shear wall systems designed and tested under unidirectional motions on the outdoor shake table in the NHERI (Natural Hazards Engineering Research Infrastructure) facility at the University of California San Diego. Each specimen had two T-walls as the main seismic force resisting system. Specimen 2 had six additional rectangular walls with their planes oriented perpendicular to the direction of the shake-table motion. They are

referred to as the out-of-plane walls in this paper. One of the objectives of the tests was to investigate the influence of the out-of-plane walls on the seismic resistance of a wall system. To this end, the T-walls in the two specimens had the same design and carried the same gravity load, and the two specimens had the same effective seismic weight.

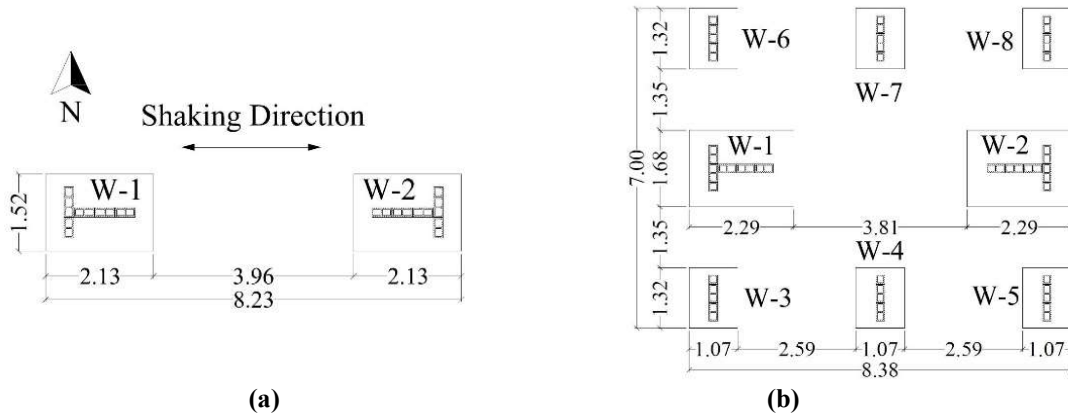


**Figure 1: Plan views of footing and wall layout (in meters): (a) Specimen 1; (b) Specimen 2**

Figure 2 shows the reinforcement details for the two specimens. The reinforcing bars in the walls had a nominal yield strength of 414 MPa (60 ksi). Each T-wall had six No. 4 (13 mm) vertical bars spaced at 20 cm (8 in) on center in the web, and three No. 4 (13 mm) vertical bars spaced at 41 cm (16 in) in the flange. The horizontal bars in the web and the flange were No. 3's (10 mm) spaced at 41 cm (16 in) on center. In Specimen 2, each of the out-of-plane walls had No. 4 (13 mm) bars for the vertical reinforcement, and No. 3 (10 mm) bars for the horizontal reinforcement, both spaced at 41 cm (16 in) on center. The reinforcement complied with the prescriptive requirements of TMS 402/602 [1] for walls designed for high seismic areas, but the spacing of the reinforcing bars in the flanges of the T-walls slightly violated the maximum spacing requirement (which is no greater than one-third of the wall length). The vertical reinforcement ran continuously from the walls into the footings, and each bar ended with a 90-degree standard hook in the footing conforming to the ACI 318-14 specification [7] for the development of reinforcement in tension. The surface of the concrete footing underneath each wall was intentionally roughened to increase the frictional resistance.

As shown in Figure 2, the roof slab of Specimen 1 consisted of 25-cm-thick (10-in) precast prestressed hollow-core planks with a 13-cm-thick (5-inch) cast-in-place concrete topping. Two reinforced concrete slabs, each with dimensions of  $3.0 \times 3.0 \times 0.36$  m (10 ft  $\times$  10 ft  $\times$  14 in), were secured on top of the roof slab to achieve the target roof mass. For Specimen 2, the roof slab consisted of 20-cm-thick (8-in) hollow-core planks with a 7.6-cm (3-in) concrete topping. It had four additional concrete slabs, each with dimensions of  $5.0 \times 3.0 \times 0.25$  m (16.5 ft  $\times$  10 ft  $\times$  10 in), as added mass. The resulting roof weights of Specimens 1 and 2, including the added concrete slabs, were 245 kN (55.1 kips) and 601 kN (135 kips), respectively. The roof weights of the two specimens were so determined that the T-walls in the two specimens carried the same gravity load. Since the roof slabs were very stiff, the tributary roof load,  $P$ , on each wall was assumed to be

proportional to the axial stiffness of the wall. The axial compressive load ratio,  $P/f'_m A_g$ , for each T-wall was 0.016, where  $A_g$  is the cross-sectional area of the wall. The compressive strength of masonry,  $f'_m$ , was specified to be 17 MPa (2.5 ksi). Including the weight of the masonry walls from the mid-height to the top, Specimen 1 had an actual seismic weight of 268 kN (60 kips), while Specimen 2 had 661 kN (149 kips). To have the same effective seismic weight as Specimen 2, the input ground motions for Specimen 1 were scaled in time and amplitude to meet the dynamic similitude requirement.

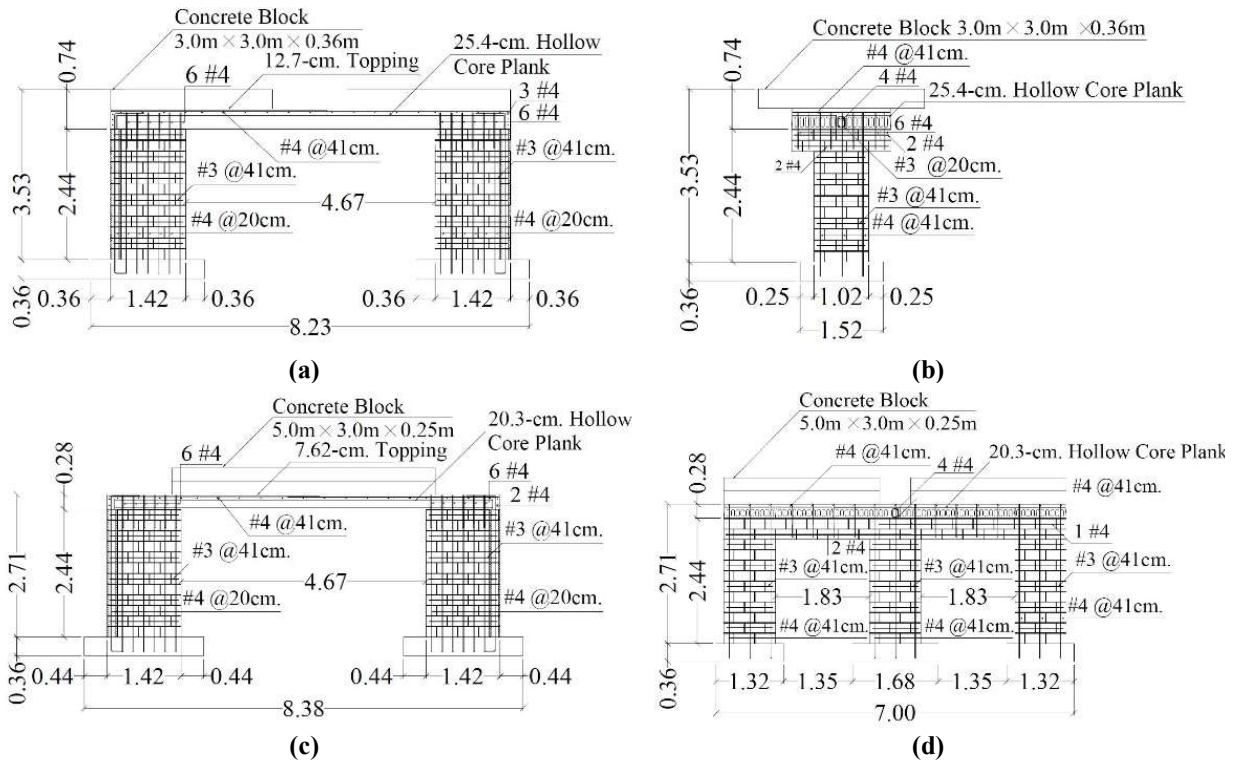


**Figure 2: Reinforcement details (in meters unless indicated): (a) South elevation view of Specimen 1; (b) West elevation view of Specimen 1; (c) South elevation view of T-walls in Specimen 2; (d) West elevation view of Specimen 2**

The flexural, diagonal shear, and sliding shear strengths of the T-walls were calculated based on the recommendations and formulas in TMS 402/602 [1] to ensure that the walls would develop diagonal shear-dominated behavior. The flexural strength was calculated using an axial force-moment interaction diagram. It was assumed that the T-walls had a fixed-fixed end condition due to the high stiffness of the roof diaphragms. The calculated flexural, diagonal shear, and sliding shear strengths were 355 kN (80 kips), 326 kN (73 kips), and 397 kN (89 kips), respectively, based on the masonry compressive strength of 17 MPa (2.5 ksi), and the expected yield strength of 469 MPa (68 ksi) for the reinforcing bars. Detailed finite element analyses [8] were conducted to facilitate the design of the specimens to ensure that the capacity of the table would be sufficient to induce collapse. Analyses were also conducted to determine the scaling of the ground motion sequences used in the tests.

## TEST SETUP AND LOADING PROTOCOL

Figure 3 shows the two specimens with their footings secured on the shake table with post-tensioned rods. The table motion was in the east-west direction. For each specimen, four concrete pedestals, with two on each of the north and south sides, were used as a catch system to prevent the free fall of the roof slab onto the table in case the walls lost their vertical load carrying capacity.

Two ground motion records from the 1994 Northridge Earthquake were selected for the shake-table tests: a far-field record from the Mulholland station (abbreviated as MUL) and a near-fault record from the Rinaldi station (abbreviated as RIN). After each earthquake motion, the specimen was subjected to white-noise excitation to identify any change in its natural period. The white noise had a root-mean-square amplitude of 0.03g and a duration of 3 minutes.

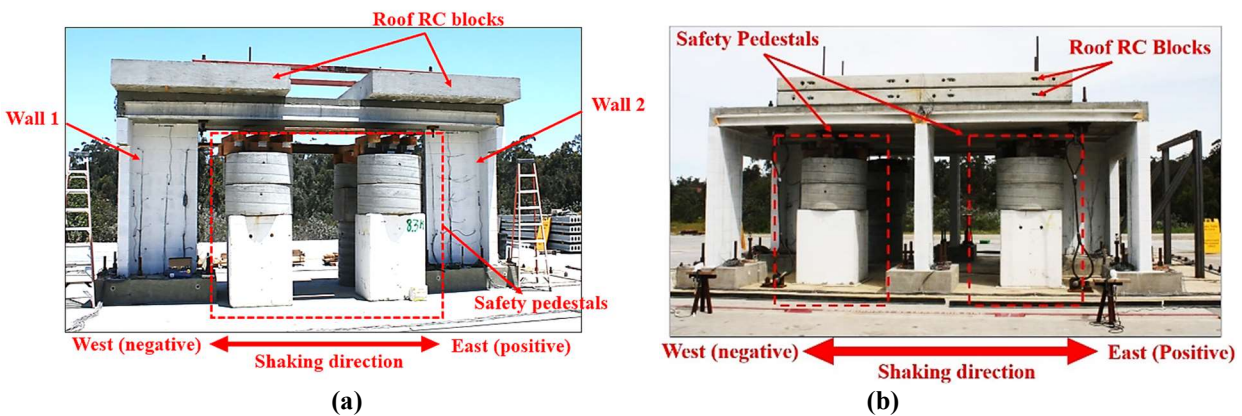


**Figure 3: Shake-table test setups: (a) Specimen 1; (b) Specimen 2**

Table 1 shows the sequences of input ground motions applied to the two specimens. Specimen 1 was tested in two phases. In the first phase, the structure was subjected to a sequence of seven Mulholland records with the acceleration scaled to 45%, 90%, 120%, and 133% of that of the original record. In the second phase, the damaged structure was subjected to a quasi-static lateral load with the test setup shown in Figure 4. Two cables were used to pull the roof slab by moving the table away from a stiff steel reaction tower, to which the other ends of the cables were attached. During the quasi-static test, the lateral load was monitored with two load cells. The horizontal roof displacement was increased until the lateral resistance of the tested structure dropped close to zero. Specimen 2 was tested with a sequence of ground motions until the structure was on the verge of collapse. The Mulholland record was used in the first six runs, with the acceleration scaled to 45%, 90%, 120%, 133%, and 160% of that of the original record. For the last run, the Rinaldi record was used with an intensity scaling of 130%. For Specimen 1, the Mulholland record was used for all the runs. As shown by the acceleration response spectrum of the record in Figure 5(a), the spectrum has a peak near 0.6 sec. It became increasingly demanding as the specimen softened due to damage. Therefore, it was a demanding record for the test sequence as long as the structural period remained below 0.6 sec., but it does not have many cycles of strong shaking as shown in Figure 5(b). For Specimen 2, the Mulholland record was used except for the last run for the same reason mentioned above. For the last run, the Rinaldi record was selected because the fundamental

period of the structure showed a significant elongation (to 0.328 s) after the sixth run, and there was a chance that the record would lose its intensity once the structural period exceeded 0.6 sec. The acceleration response spectrum of the Rinaldi record has a more or less uniform intensity in the period range of 0.3 to 0.7 s, and the intensity drops gently afterwards.

**Table 1: Test Sequences for Specimens 1 and 2**

Test ID	1	2	3	4	5	6	7	8
Specimen 1	MUL-45%	MUL-45%	MUL-90%	MUL-90%	MUL-90%	MUL-120%	MUL-133%	Static Pull*
Specimen 2	MUL-45%	MUL-90%	MUL-120%	MUL-90%	MUL-133%	MUL-160%	RIN-130%*	-

\* No white-noise test was performed because of the damage state of the specimens.

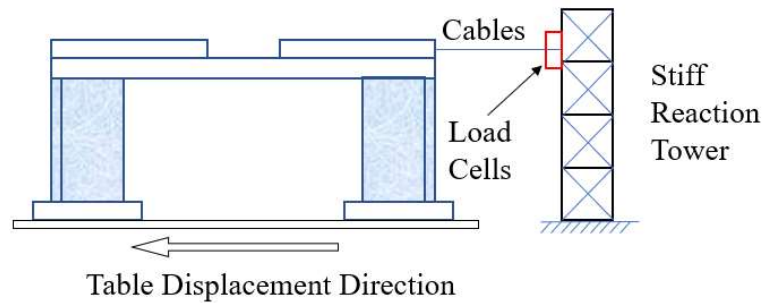


**Figure 4: Pull test setup for Specimen 1**

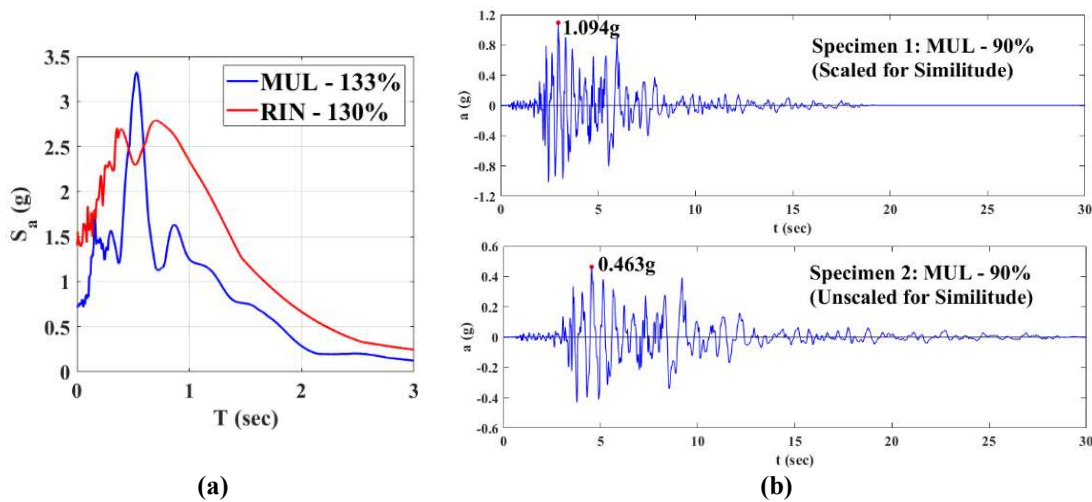


**Figure 5: Table motions recorded in shake-table tests: (a) Acceleration spectra of MUL-133% and RIN-130% from the tests of Specimen 2; (b) Acceleration histories for MUL-90% from the tests of Specimens 1 and 2**

Since Specimens 1 and 2 had different roof weights, as mentioned before, additional scaling was applied to the time and amplitude of the earthquake records used for Specimen 1 to attain the dynamic similitude between the two specimens. The ground acceleration was scaled up by a factor

of  $S_a = 2.4$  (seismic weight of Specimen 2 / seismic weight of Specimen 1), and the time was compressed by a factor of  $\sqrt{1/S_a} = 0.65$ , with the assumption that both structures had the same lateral stiffness and strength as would be the case in design practice. Figure 5(b) shows the table acceleration histories for the 90%-level Mulholland records obtained from two tests performed on Specimens 1 and 2, respectively.

## TEST RESULTS

This section presents the major observations and the structural response obtained from the tests of the two specimens with the wall numbers identified in Figure 1. For both specimens, the roof drift ratios were calculated as the relative roof displacement divided by the wall height of 2.44 m (8 ft). The base shear was calculated as the product of the average roof acceleration along the shaking direction, measured by the accelerometers installed along the perimeter of the roof slabs, and the seismic mass consisted of the total roof mass and the masonry mass above the mid-height of the walls.

### *Specimen 1*

Two low-intensity and three mid-intensity tests were conducted on Specimen 1 by scaling the Mulholland record to 45% and 90%, respectively, as shown in Table 1. After three shakings with the 90%-level motions, it was observed that a few hairline flexural cracks initiated in the webs near the bottom of the two walls. The strain monitored by the strain gauges installed on the reinforcing bars showed that the vertical bars at the two extreme sides of the webs of the two T-walls yielded in tension near the wall base. Moreover, three (out of six) vertical bars in the flanges had yielded at the first masonry course from the base.

During the test with the 120%-level Mulholland motion, hairline cracks occurring in the last few tests opened and extended. Meanwhile, more flexural cracks initiated and propagated in the webs and flanges near the bottom of both walls. As shown in Figure 6(a), during this motion, the maximum resistance developed by the structure reached 598 kN (134 kips) at a roof drift ratio of 0.35%. The maximum roof drift ratio reached in this test was 0.47%.

The last dynamic test on Specimen 1 was conducted with a 133%-level Mulholland motion. In this test, the walls developed severe shear cracks. Figure 7 shows the severe diagonal shear cracks and the masonry spalling and crushing that developed in the webs of the T-walls. Wall-2 (East T-Wall) also showed base crushing and subsequent buckling of the extreme vertical bar in the web near the wall base. The base shear-vs.-roof drift hysteresis curves for the structure (Figure 6) shows that the peak strength of 690 kN (155 kips) was reached at a roof drift ratio of about 1% in the negative (west) direction. The peak strength of the specimen is close to the shear strength of 685 kN calculated with the formula given in TMS 402/602 [1]. The masonry compressive strength and the yield strength of the horizontal reinforcing bars used in the strength calculation were the average strengths obtained from the material sample tests. They are 20 MPa (2.9 ksi) and 521 MPa (75.6 ksi), respectively. A maximum roof drift ratio of 2.53% was reached in the west direction. At this drift level, the lateral resistance of the tested structure dropped to 340 kN (76.3 kips), which was

about 50% of the peak strength. After this test, most of the vertical and horizontal bars in the webs yielded at the locations where the major diagonal cracks developed.

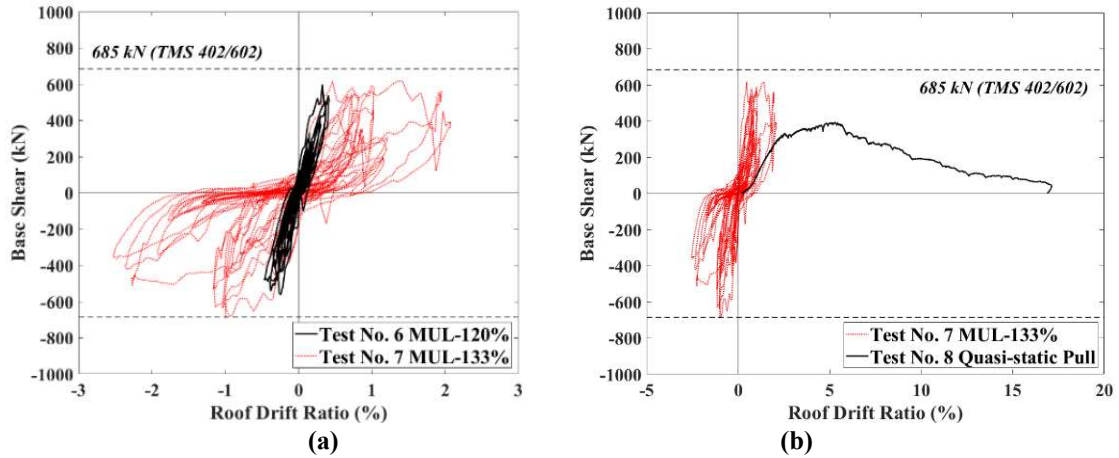


**Figure 6: Base shear-vs.-roof drift ratio curves for Specimen 1: (a) Responses from the ground motion tests; (b) Results from the quasi-static and last ground motion tests**



**Figure 7: Damage in Specimen 1 after MUL-133%: (a) South view of Wall-1; (b) North view of Wall-2**

After MUL-133%, to examine the maximum roof drift ratio that could be sustained by the structure before collapse, a quasi-static test was conducted by pulling the roof with steel cables. During the quasi-static test, the diagonal cracks in each wall continued to extend and open as the horizontal roof displacement increased. Severe crushing and spalling of the masonry were observed. Fracture occurred in two horizontal bars at the locations of major diagonal crack opening during the quasi-static test. As shown in Figure 6(b), the lateral resistance of the wall system dropped to 44 kN (9.9 kips), which is 6% of the peak strength, when a roof drift ratio of 16.7% (42.4-cm roof horizontal displacement) was reached. As shown in Figure 8, at the roof drift ratio level of 16.7%, collapse was averted because the flanges were still able to carry the weight of the roof slab when the masonry in the wall webs had been severely crushed.





**Figure 8: Damage in Specimen 1 after the quasi-static pull test**

***Specimen 2***

Specimen 2 was subjected to a similar sequence of ground motions as Specimen 1, which were 45%, 90%, 120% and 133%-level Mulholland motions, as shown in Table 1. While flexural and shear cracks developed in Specimen 1 after the 120% and 133%-level Mulholland motions, there were no visible cracks observed in Specimen 2 after the MUL-133%. Figure 9(a) shows the base shear-vs.-roof drift ratio curves for the MUL-133% motion applied to Specimen 2. The peak drift ratio reached in the test was 0.25%, while the maximum base shear developed was 726 kN (163 kips).

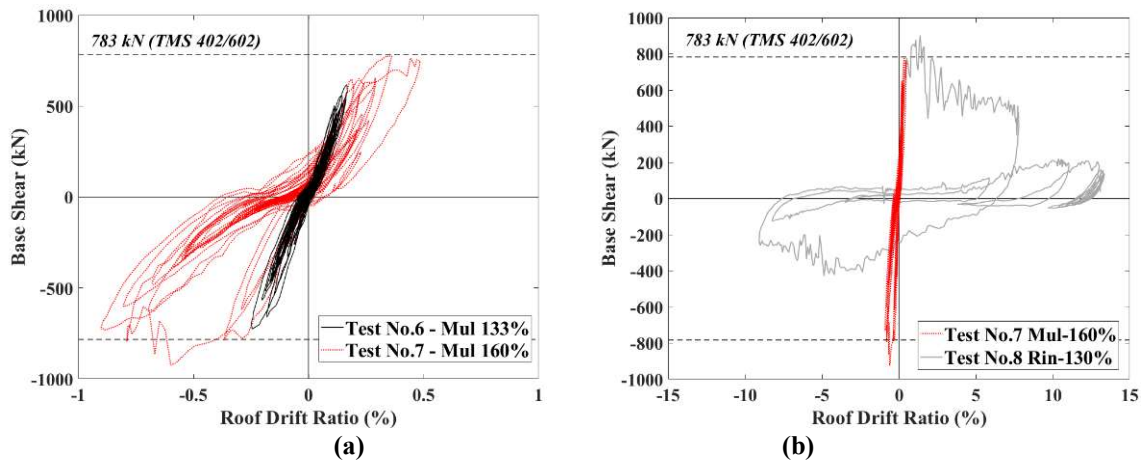


**Figure 9: Base shear-vs.-roof drift ratio curves for Specimen 2: (a) Mulholland motions; (b) last two motions**

During MUL-160%, a maximum drift ratio of 0.90% was reached. As shown in Figure 9, the base shear capacity of 925 kN (208kips) was reached at a roof drift ratio of 0.60% in the negative (west) direction. During the test, degradation of lateral resistance was relatively mild, about 22% with respect to the peak. Flexural and diagonal shear cracks occurred in the webs of the two T-walls, and toe crushing occurred in the web of Wall-2. With the initiation of diagonal cracks in the webs of the two T-walls, yielding occurred in the vertical and horizontal bars at locations intersected by diagonal shear cracks.

During RIN-130%, Specimen 2 reached verge of collapse with a maximum drift ratio of 13.4%. Severe damage was developed on the web of two T-walls. The base shear-vs.-roof drift ratio curves in Figure 9(b) show that the maximum base shear reached 902 kN (203 kips) at a drift ratio of 1.39% in the positive (east) direction. The specimen developed a residual strength of 185 kN (41.6 kips), which was about 20% of the peak strength (208 kips) reached during MUL-160%. Figure 10 shows the damage of the specimen after the test. The diagonal cracks developed during MUL-160% extended further and were accompanied by the opening of new diagonal cracks in the webs of the T-walls. As in the quasi-static test of Specimen 1, severe masonry crushing occurred in the wall webs. After this test, all the horizontal bars (except the two top bars) in the webs of the T-walls fractured at the locations along the major shear cracks. The webs and flanges of the T-walls were practically separated. The failure of the 90-degree hooks connecting the flanges and webs was observed, along with the fracture of the horizontal bars crossing the flange-web interfaces. The flanges of the T-walls exhibited severe out-of-plane bending at the elevation of the horizontal cracks that developed in motion MUL-160%. However, the roof slab remained practically intact during the test. At the end of the tests, the webs of the T-walls in both specimens had lost significant portions of the masonry due to crushing, and the roof weight was carried by the wall flanges and the out-of-plane walls.

For Specimen 2, the predicted lateral strength given by the formula in TMS 402/602 [1] is 783 kN, which is 15.4% less than the maximum base shear obtained during tests. In the calculation, the lateral resistance of Specimen 2 is assumed to be provided by the two T-walls only, and the flexural resistance of the six out-of-plane walls is ignored. The average masonry compressive strength and yielding strength of horizontal reinforcing steel used in the calculation are 27 MPa (3.9 ksi) and 523 MPa (75.9 ksi), respectively. The higher peak lateral resistance during the tests can be attributed to the axial restraint introduced by the six out-of-plane walls. As the T-walls developed flexural deformation, they rocked on the footings because of the penetration of the tensile strains in the vertical bars into the region embedded in the footings. The rocking motion of the walls would push up the roof diaphragm, which was, however, restrained from moving up by the out-of-plane walls. Hence, the T-walls experienced increased axial compression when they rocked due to the restraint of the out-of-plane walls.



**Figure 10: Damage in Specimen 2 after RIN-130%: (a) South view of Specimen 2; (b) South view of Wall-1; (c) South view of Wall-2**

## CONCLUSIONS

This paper presents a study to investigate the collapse resistance of shear-dominated, fully grouted, RM wall systems designed for high seismic areas. Two single-story specimens, each having two RM T-walls as the seismic load resisting system, were tested on a shake table. Specimen 2 had six additional planar walls (out-of-plane walls) perpendicular to the direction of shaking. Specimen 1 was first tested with a sequence of earthquake ground motions, and was finally subjected to quasi-static loading to the verge of collapse. The T-walls exhibited flexural behavior with the yielding of the vertical reinforcement during lower level earthquake motions, but had failures eventually dominated by diagonal shear cracks. The maximum lateral resistance developed is close to the shear strength calculated with the formula in TMS 402/602 [1] based on the assumption that the axial force in each wall is due to the gravity load only. In the quasi-static test, the roof diaphragm was pulled to a maximum drift of 16.7%, at which the lateral resistance of the wall system dropped to 6% of the peak strength; but the structure did not collapse.

Specimen 2 was tested with a sequence of earthquake ground motions up to the verge of collapse. Compared to Specimen 1, Specimen 2 had a higher lateral resistance and had first cracks observed at a higher intensity ground motion. The specimen survived the last motion without collapse. The maximum roof drift reached 13.4%, at which the residual strength dropped to 20% of the peak strength. Specimen 2 developed higher maximum lateral resistance than the shear strength calculated by the formula in TMS 402/602 [1], which can be attributed to the additional axial compression exerted on the T-walls by the out-of-plane walls when the former rocked.

The two test specimens exhibited significantly higher displacement capacities than shear-dominated planar wall segments tested in previous studies under quasi-static cyclic loads. The higher displacement capacities can be largely attributed to the presence of wall flanges and, for the case of Specimen 2, the out-of-plane walls, which provided an alternative load path to carry the gravity load when the webs of the T-walls had been severely damaged.

## ACKNOWLEDGEMENTS

This project was supported with funding from the National Science Foundation (NSF) under Award No. CMMI-1728685. The support of the NHERI program of the NSF for the shake-table tests conducted at UC San Diego is also gratefully acknowledged. The authors are grateful to the support of RCP Block and Brick, Concrete Masonry Association of California and Nevada, Masonry Institute of America, and Northwest Concrete Masonry Association. However, opinions expressed in this paper are those of the authors and do not necessarily reflect those of the sponsors.

## REFERENCES

- [1] TMS 402/602. (2016). *Building Code Requirements for Masonry Structures*. The Masonry Society, Boulder, CO.
- [2] Voon, K. C. and Ingham, J. M. (2006). "Experimental in-plane shear strength investigation of reinforced concrete masonry walls." *J Struct Eng*. 132(3):400-8.

- [3] Shing, P. B., Noland, J. L., Spaeh, H. P., Klamerus, E. W., and Schuller, M. P. (1991) *Response of single-story reinforced masonry shear walls to in-plane lateral loads*. Department of Civil, Environmental and Architectural Engineering University of Colorado, Boulder, CO.
- [4] Ahmadi, F. (2012). *Displacement-based seismic design and tools for reinforced masonry shear-wall structures*. Ph.D. Dissertation, Department of Civil Engineering, University of Texas at Austin, Austin, TX.
- [5] Mavros, M., Ahmadi, F., Shing, P. B., Klingner, R. E., McLean, D., and Stavridis, A. (2016) "Shake-table tests of a full-scale two-story shear-dominated reinforced masonry wall structure." *J Struct Eng*. 142(10):04016078.
- [6] Stavridis, A., Ahmadi, F., Mavros, M., Shing, P. B., Klingner, R. E., and McLean, D. (2016) "Shake-table tests of a full-scale three-story reinforced masonry shear wall structure." *J Struct Eng*. 142(10):04016074.
- [7] ACI Committee. (2014). *Building Code Requirements for Structural Concrete (ACI 318-14) and Commentary (ACI 318R-14)*. American Concrete Institute, Farmington Hills, MI.
- [8] Koutras A. A. (2019) *Assessment of the seismic behavior of fully and partially grouted reinforced masonry structural systems through finite element analysis and shake-table testing*. Ph.D. Dissertation, University of California San Diego, La Jolla, CA.